1st International Conference on Multidisciplinary Engagement

Stability of the Augmented Solow Model with Physical and Human Capital Diffusion

Dinda Laura Putri Permadi[1*], Sutrima[2], Siswanto[3]
[1,2,3]*Department of Mathematics, Faculty of Mathematics and Natural Sciences, Sebelas Maret University, Jl. Ir. Sutami 36 A Kentingan Surakarta 57126, Central Java, Indonesia*

Corresponding Author.
**Email*: dindalaura@student.uns.ac.id

Abstract: This study formulates the augmented Solow model as a two-component reaction–diffusion system, governing the spatial dynamics of physical and human capital per effective unit of labor. The analysis examines the local asymptotic stability of the positive steady state, the effect of spatial capital diffusion on stability properties, and the possibility of Turing and Hopf bifurcations under decreasing returns to scale. Stability is analyzed using linearization and Jacobian-based stability criteria, including the Routh–Hurwitz conditions, for both the non-spatial and spatial systems. The spatial Jacobian is shown to satisfy a strictly negative trace and a strictly positive determinant for all nonnegative wave numbers, confirming that the steady state remains locally asymptotically stable. Bifurcation analysis further establishes that neither Turing nor Hopf instabilities arise, demonstrating that spatial diffusion does not destabilize the balanced growth path. Numerical simulations using a forward Euler finite-difference scheme illustrate convergence of both capital variables to the steady state under simultaneous localized perturbations. These results indicate that, for initial conditions within a neighborhood of the steady state, the joint mobility of physical and human capital supports convergence toward the homogeneous balanced growth path, with each spatial mode decaying toward the steady state, while decreasing returns to scale prevent persistent spatial disparities and oscillatory behavior.
Keywords: augmented Solow model, reaction–diffusion, stability, bifurcation, balanced growth path

1. INTRODUCTION

Persistent disparities in per-capita income across regions remain a central topic in growth economics. Empirical studies attribute these differences, at least in part, to the uneven spatial distribution of production factors, particularly physical capital and human capital [1, 2]. Physical capital tends to concentrate in more productive regions, while skilled workers migrate toward areas offering higher returns to education, potentially reinforcing regional income inequality [3, 4]. In standard neoclassical growth models, however, each economy is treated as a spatially homogeneous unit that evolves independently, abstracting from factor mobility and interregional interactions. At the regional level, this assumption becomes untenable, as spatial interactions may alter the stability properties of the long-run steady state [5, 6].

The neoclassical theory of economic growth was developed by Solow [7] and Swan [8], with output modeled as a function of capital and labor under a Cobb–Douglas production technology exhibiting diminishing marginal returns to capital. Under these assumptions and Harrod-neutral technological progress, the model converges to a unique positive steady state along a balanced growth path. Mankiw et al. [9] extended the Solow–Swan model by introducing human capital as a second accumulable input alongside physical capital. This extension, known as the augmented Solow model, assumes decreasing returns to scale in the two accumulable capital inputs, which preserves the convergence properties of the original model while substantially improving empirical performance, explaining approximately 80 percent of the cross-country variation in per capita income [9].

Several studies have therefore incorporated spatial mechanisms into neoclassical growth models. Since capital tends to flow from capital-abundant regions toward capital-scarce regions, the spatial dynamics of mobile capital can be naturally described by a reaction–diffusion system. Camacho and Zou [10] analyzed the existence and convergence of solutions to a spatially extended Solow system, while Capasso et al. [11] formulated a reaction–diffusion model in which physical capital is the only mobile factor. Xepapadeas and Yannacopoulos [12] studied nonlinear diffusion driven by productivity gradients, and González-Parra et al. [13] analyzed the

effects of boundary conditions on capital flow dynamics. Juchem Neto et al. [14] further showed that spatial capital mobility may generate economic agglomeration. However, these studies restrict attention to physical capital diffusion and do not account for the accumulation and spatial diffusion of human capital.

Spatial diffusion has also been shown to significantly influence stability and pattern formation in growth models. Fischer [15] examined knowledge diffusion across regions, while Aymard [16], Ureña and Vargas [17], Zhong and Huang [18], and Zhong [19] analyzed stability and spatial dynamics in reaction–diffusion growth systems. Most relevant to the present research, Kong et al. [20] identified conditions for Hopf bifurcations generated by capital-induced labor migration, and Li et al. [21] established conditions for Turing instability in a spatial Solow model with a single capital variable. Although these contributions demonstrate that spatial diffusion can substantially alter stability properties, none examines how the interaction between physical and human capital diffusion jointly shapes the stability and bifurcation conditions of the augmented Solow model.

To address this gap, the present research formulates the augmented Solow model as a two-component reaction–diffusion system for physical capital $k(x,t)$ and human capital $h(x,t)$ per effective unit of labor:

$$\begin{aligned} k_t(x,t) &= s_k\, k(x,t)^{\alpha} h(x,t)^{\beta} - \mu\, k(x,t) + D_k\, k_{xx}(x,t), \qquad (x,t) \in (0,L) \times (0,\infty), \\ h_t(x,t) &= s_h\, k(x,t)^{\alpha} h(x,t)^{\beta} - \mu\, h(x,t) + D_h\, h_{xx}(x,t), \qquad (x,t) \in (0,L) \times (0,\infty), \end{aligned} \tag{1}$$

with initial and homogeneous Neumann boundary conditions,

$$\begin{aligned} k(x,0) &= k_0(x), \;\; h(x,0) = h_0(x), \qquad x \in \Omega, \\ k_x(0,t) &= k_x(L,t) = h_x(0,t) = h_x(L,t) = 0, \qquad t > 0, \end{aligned} \tag{2}$$

ensuring zero capital flux across domain boundaries. Here, s_k, s_h, α, β, D_k, D_h and $\mu := n + g + \delta$ denote the saving rates, output elasticities, diffusion coefficients, and effective depreciation rate for physical and human capital, where $n, g,$ and δ represent population growth, technological progress, and capital depreciation, respectively. The condition $\alpha + \beta < 1$ imposes decreasing returns to scale on the two accumulable capital inputs. The remaining parameters satisfy $s_k,\ s_h \in (0,1)$; $\alpha, \beta > 0$; and $n,\ g,\ \delta > 0$.

Accordingly, this research aims to analyze the local asymptotic stability conditions of the non-spatial steady state of the augmented Solow model [22], to determine whether the spatial diffusion of physical and human capital alters the stability properties of the system [23, 24], and to examine the possibility of Turing and Hopf bifurcations arising in the associated two-component reaction–diffusion model [25, 26]. The remainder of the paper is organized as follows. Section 2 presents the research methods and procedure. Section 3 presents the main results, comprising the stability analysis of both the non-spatial and spatial systems, bifurcation analysis, and supporting numerical simulations. Section 4 concludes the paper and outlines directions for future research.

2. METHOD

This research employs literature review and numerical simulation. The augmented Solow model is formulated as a two-component reaction–diffusion system, and its unique positive steady state is obtained in closed form from the stationary conditions. Local asymptotic stability is analyzed by linearizing the system around the steady state and evaluating the Jacobian matrix. The Routh–Hurwitz conditions on the trace and determinant of the mode-dependent Jacobian are used to assess stability in both the non-spatial system and all spatial modes from the Fourier cosine expansion under homogeneous Neumann boundary conditions. Conditions for Turing and Hopf bifurcations are then derived from the sign of the mode-dependent trace and determinant. Numerical simulations with a forward Euler finite-difference scheme illustrate the analytical results for a representative parameter set. The parameters satisfy the model's admissibility conditions and align with plausible macroeconomic values in the literature [9]. The research procedure is shown in Figure 1.

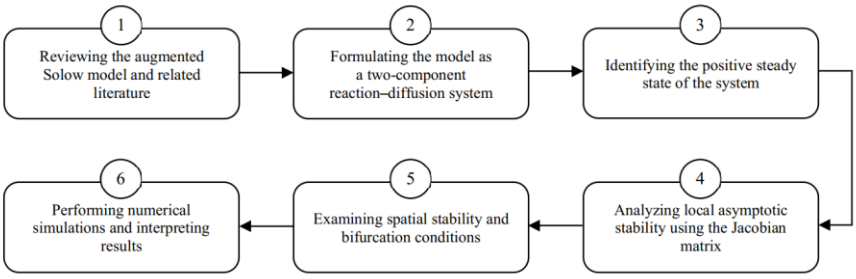

Figure 1. Research procedure

3. RESULTS AND DISCUSSION

3.1 Stability Analysis of the Non-Spatial Model

This subsection establishes the local asymptotic stability of the positive steady state of the non-spatial augmented Solow model of Mankiw et al. [9]. The system is governed by the following two-dimensional system of ordinary differential equations:

$$\begin{aligned} \dot{k}(t) &= s_k k(t)^{\alpha} h(t)^{\beta} - \mu k(t), \\ \dot{h}(t) &= s_h k(t)^{\alpha} h(t)^{\beta} - \mu h(t). \end{aligned} \tag{3}$$

where $k(t)$ and $h(t)$ denote physical and human capital per effective unit of labor, respectively. System (3) describes the spatially homogeneous dynamics of system (1) and its positive steady state E^* serves as the reference point for the stability analysis in Section 3.2.

A nontrivial steady state (k^*, h^*) satisfies

$$f(k,h) \coloneqq s_k k^{\alpha} h^{\beta} - \mu k = 0, \qquad g(k,h) \coloneqq s_h k^{\alpha} h^{\beta} - \mu h = 0. \tag{4}$$

The trivial steady state $(0,0)$ is discarded, as an economy without capital accumulation is economically irrelevant. System (3) admits a unique positive nontrivial steady state for $k > 0$ and $h > 0$, given by,

$$E^* = \left(\left(\frac{s_k^{1-\beta} s_h^{\beta}}{\mu} \right)^{\frac{1}{1-\alpha-\beta}}, \left(\frac{s_k^{\alpha} s_h^{1-\alpha}}{\mu} \right)^{\frac{1}{1-\alpha-\beta}} \right) = (k^*, h^*),$$

where k^* and h^* denote the steady state levels of physical and human capital per effective unit of labor, respectively. The uniqueness of E^* follows from its derivation from system (4), while $\alpha + \beta < 1$ ensures that all expressions are well-defined and $\frac{1}{1-\alpha-\beta} > 0$.

Theorem 3.1 *System (3) is locally asymptotically stable at the positive steady state E^* if $\alpha + \beta < 1$.*

Proof. Evaluating the Jacobian of system (3) at E^* using the steady-state conditions (4) gives,

$$J_{E^*} = \begin{bmatrix} (\alpha - 1)\mu & \beta\mu \dfrac{k^*}{h^*} \\ \alpha\mu \dfrac{h^*}{k^*} & (\beta - 1)\mu \end{bmatrix},$$

with characteristic equation,

$$\lambda^2 - (\alpha + \beta - 2)\mu\,\lambda + (1 - \alpha - \beta)\mu^2 = 0. \tag{5}$$

From (5), the trace and determinant of J_{E^*} are

$$tr(J_{E^*}) = (\alpha + \beta - 2)\mu, \qquad \det(J_{E^*}) = (1 - \alpha - \beta)\mu^2.$$

Given that $\mu > 0$, the determinant is strictly positive if and only if $1 - \alpha - \beta > 0$, i.e., $\alpha + \beta < 1$. Under this condition, the trace is negative, $tr(J_{E^*}) < 0$. Therefore, by the Routh–Hurwitz criterion, the steady state E^* is locally asymptotically stable, which is consistent with the assumption of decreasing returns to scale $\alpha + \beta < 1$. □

Under linearization at E^*, the trace $tr(J_{E^*}) < 0$ governs the decay rate of perturbations, while the determinant $\det(J_{E^*}) > 0$, ensured by decreasing returns to scale, captures the strength of the restoring forces toward E^*. As $\alpha + \beta \to 1$, the decay rate diminishes in magnitude and the restoring forces weaken, leading to slower convergence toward the balanced growth path.

3.2 Stability Analysis of the Spatial Model

The stability of the reaction–diffusion system (1) is examined via linearization around the positive steady state E^*. Small perturbations about E^* are defined as

$$k(x,t) = k^* + u(x,t), \qquad h(x,t) = h^* + v(x,t), \tag{6}$$

where $|u(x,t)| \ll 1$ and $|v(x,t)| \ll 1$. Substituting (6) into system (1) and neglecting higher-order nonlinear terms yields the linearized system

$$u_t(x,t) = \mu(\alpha - 1)u + \left(\beta\mu\frac{k^*}{h^*}\right)v + D_k u_{xx},$$
$$v_t(x,t) = \left(\alpha\mu\frac{h^*}{k^*}\right)u + \mu(\beta - 1)v + D_h v_{xx}, \quad (7)$$

with initial and Neumann boundary conditions

$$u(x,0) = k_0(x) - k^*, \quad v(x,0) = h_0(x) - h^*, \quad x \in \Omega$$
$$u_x(0,t) = u_x(L,t) = v_x(0,t) = v_x(L,t) = 0, \quad t > 0. \quad (8)$$

The initial-boundary value problem (7)–(8) is solved by separation of variables. The perturbation functions $(u(x,t), v(x,t))$ are expanded into Fourier cosine series,

$$u(x,t) = \sum_{q=0}^{\infty} \epsilon_q(t)\, cos(qx)\ , \qquad v(x,t) = \sum_{q=0}^{\infty} \eta_q(t)\, cos(qx), \quad (9)$$

Substituting (9) into the linearized system and canceling the common basis function $cos(qx)$ for each mode q yields the system of first-order ordinary differential equations

$$\begin{bmatrix} \dot{\epsilon}_q(t) \\ \dot{\eta}_q(t) \end{bmatrix} = J_q \begin{bmatrix} \epsilon_q(t) \\ \eta_q(t) \end{bmatrix}, \quad (10)$$

where $J_q = J_{E^*} - q^2\mathbf{D}$, with

$$J_{E^*} = \begin{bmatrix} a_{11} & a_{12} \\ a_{21} & a_{22} \end{bmatrix}, \qquad \mathbf{D} = \begin{bmatrix} D_k & 0 \\ 0 & D_h \end{bmatrix},$$

and entries,

$$a_{11} = (\alpha - 1)\mu, \qquad a_{12} = \beta\mu\frac{k^*}{h^*},$$
$$a_{21} = \alpha\mu\frac{h^*}{k^*}, \qquad a_{22} = (\beta - 1)\mu.$$

Consequently, the mode-dependent matrix J_q is given by

$$J_q = \begin{bmatrix} \mu(\alpha - 1) - D_k q^2 & \beta\mu\dfrac{k^*}{h^*} \\ \alpha\mu\dfrac{h^*}{k^*} & \mu(\beta - 1) - D_h q^2 \end{bmatrix}.$$

Local stability of system (10) is governed by the eigenvalues λ_q of J_q, satisfying

$$\lambda^2 - tr(J_q)\lambda + \det(J_q) = 0,$$

where the trace and determinant are

$$tr(J_q) = tr(J_{E^*}) - tr(\mathbf{D})q^2,$$
$$\det(J_q) = \det(\mathbf{D})\, q^4 - (a_{11}D_h + a_{22}D_k)q^2 + \det(J_{E^*}). \quad (11)$$

Remark 3.1 *For $q = 0$, system (10) reduces to the linearized non-spatial system (3), and stability follows directly from Theorem 3.1. The following theorems address all $q \geq 0$.*

Theorem 3.2 *The reaction–diffusion system (1) is locally asymptotically stable at the steady state E^* for all spatial modes $q \geq 0$ provided $\alpha + \beta < 1$.*

Proof. By the Routh–Hurwitz criterion, local stability requires $tr(J_q) < 0$ and $det(J_q) > 0$. From (11), trace and determinant at E^* is

$$tr(J_q) = \mu(\alpha + \beta - 2) - (D_k + D_h)q^2,$$
$$\det(J_q) = D_k D_h q^4 - \mu[\, D_h(\alpha - 1) + D_k(\beta - 1)]q^2 + \mu^2(1 - \alpha - \beta), \quad (12)$$

Since $\alpha + \beta < 1$ implies $\alpha + \beta - 2 < 0$ and $(D_k + D_h)q^2 \geq 0$, it follows that $tr(J_q) < 0$ for all $q \geq 0$. Moreover, $det(J_q)$ is a quadratic polynomial in q^2 with strictly positive coefficients under $\alpha + \beta < 1$, hence $det(J_q) > 0$ for all $q \geq 0$. Therefore, the system is locally asymptotically stable at E^* under decreasing returns to scale, $\alpha + \beta < 1$. □

Theorem 3.3 *Let* (k^*, h^*) *be an asymptotically stable steady state of system (1). Then, under homogeneous Neumann boundary conditions, the solution* $\big(k(x,t), h(x,t)\big)$ *satisfies*

$$lim_{t\to\infty}\big(k(x,t), h(x,t)\big) = (k^*, h^*).$$

Proof. Using the perturbation definition (6), it suffices to show $lim_{t\to\infty}\big(u(x,t), v(x,t)\big) = (0,0)$. Expanding the perturbations into an orthogonal Fourier cosine series in $L^2(0,L)$ yields

$$u(x,t) = \sum_{n=0}^{\infty} \epsilon_n(t)\, cos(\kappa_n x)\ , \qquad v(x,t) = \sum_{n=0}^{\infty} \eta_n(t)\, cos(\kappa_n x),$$

where the admissible wave numbers $\kappa_n = \frac{n\pi}{L}$ for $n = 0,1,2,\ldots$, arise from the Neumann boundary conditions, corresponding to the q in the expansion (9). The temporal and spatial derivatives satisfy

$$\begin{aligned} u_t &= \sum_{n=0}^{\infty} \dot{\epsilon}_n(t)\, cos(\kappa_n x), \qquad u_{xx} = -\sum_{n=0}^{\infty} \kappa_n^2 \epsilon_n(t)\, cos(\kappa_n x), \\ v_t &= \sum_{n=0}^{\infty} \dot{\eta}_n(t)\, cos(\kappa_n x), \qquad v_{xx} = -\sum_{n=0}^{\infty} \kappa_n^2 \eta_n(t)\, cos(\kappa_n x), \end{aligned} \tag{13}$$

Substituting (13) into system (7) and exploiting the orthogonality of $cos(\kappa_n x)$, the system decouples into ordinary differential equations for each spatial mode $n \geq 0$,

$$\begin{aligned} \dot{\epsilon}_n(t) - (a_{11} - D_k\kappa_n^2)\epsilon_n(t) &= a_{12}\eta_n(t), \\ \dot{\eta}_n(t) - (a_{22} - D_h\kappa_n^2)\eta_n(t) &= a_{21}\epsilon_n(t) \end{aligned}$$

Applying integrating factors $I_n^{\epsilon}(t) = e^{-(a_{11} - D_k\kappa_n^2)t}$ and $I_n^{\eta}(t) = e^{-(a_{22} - D_h\kappa_n^2)t}$, the solutions are expressed as

$$\epsilon_n(t) = \epsilon_n(0)e^{(a_{11} - D_k\kappa_n^2)t} + a_{12}\int_0^t e^{(a_{11} - D_k\kappa_n^2)(t-\tau)}\eta_n(\tau)d\tau,$$

$$\eta_n(t) = \eta_n(0)e^{(a_{22} - D_h\kappa_n^2)t} + a_{21}\int_0^t e^{(a_{22} - D_h\kappa_n^2)(t-\tau)}\epsilon_n(\tau)d\tau,$$

Since $a_{11} < 0$ and $a_{22} < 0$ by Theorem 3.1, and $D_k, D_h > 0$, the exponents $(a_{11} - D_k\kappa_n^2)$ and $(a_{22} - D_h\kappa_n^2)$ are strictly negative for all $n \geq 0$. Both solutions therefore decay exponentially, giving

$$lim_{t\to\infty}\, \epsilon_n(t) = 0, \qquad lim_{t\to\infty}\, \eta_n(t) = 0, \qquad \forall n.$$

By uniform convergence of the Fourier series,

$$lim_{t\to\infty}\, u(x,t) = 0, \qquad lim_{t\to\infty}\, v(x,t) = 0, \qquad x \in [0,L],$$

and hence, the solutions of the spatial system (1) converge asymptotically to the steady state,

$$lim_{t\to\infty}\big(k(x,t), h(x,t)\big) = (k^*, h^*).$$ □

Theorems 3.2 and 3.3 establish that diffusion does not destabilize the steady state at the level of the linearized dynamics. Since $q^2 \geq 0$ and **D** is positive definite, the term $-q^2\mathbf{D}$ shifts the spectrum of J_{E^*} strictly to the left for all $q > 0$, increasing the decay rate of spatial perturbations relative to the non-spatial case. Thus, capital mobility supports local convergence without inducing instability under $\alpha + \beta < 1$.

3.3 Bifurcation Analysis

This subsection examines whether the introduction of spatial diffusion can destabilize the balanced growth path of the augmented Solow model. Instabilities in system (1) may arise if the trace or determinant of the mode-dependent Jacobian J_q satisfies $tr(J_q) \geq 0$ or $det(J_q) \leq 0$ for certain spatial modes q. Since the trace is strictly negative under $\alpha + \beta < 1$ (Theorem 3.2), the possibility of diffusion-induced instability is determined entirely by the sign of $det(J_q)$.

Specifically, a Turing bifurcation requires: (i) E^* is stable in the non-spatial system, and (ii) $det(J_q) < 0$ for some $q > 0$, so that diffusion destabilizes a spatial mode. A Hopf bifurcation requires $tr(J_q) = 0$ and

$det(J_q) > 0$ for some $q \geq 0$, signaling the onset of temporally oscillatory solutions. The following theorems show that neither condition is attainable under $\alpha + \beta < 1$

Theorem 3.4 *The reaction–diffusion system (1) does not exhibit Turing bifurcation at the steady state E^* provided $\alpha + \beta < 1$.*

Proof. Turing instability requires $det(J_q) < 0$ for some $q > 0$. From (12), the determinant is

$$\det(J_q) = D_k D_h q^4 - \mu[D_h(\alpha - 1) + D_k(\beta - 1)]q^2 + \mu^2(1 - \alpha - \beta).$$

It suffices to show that all three coefficients of this polynomial in q^2 are strictly positive under $\alpha + \beta < 1$. The leading coefficient $D_k, D_h > 0$ and the constant term $\mu^2(1 - \alpha - \beta) > 0$ follow immediately. For the coefficient of q^2, since $\alpha + \beta < 1$ with $\alpha, \beta > 0$, it follows that $\alpha < 1$ and $\beta < 1$, hence $(1 - \alpha) > 0$ and $(1 - \beta) > 0$. Consequently,

$$-\mu[D_h(\alpha - 1) + D_k(\beta - 1)] = \mu[(1 - \alpha)D_h + (1 - \beta)D_k] > 0.$$

Therefore, all coefficients are strictly positive, implying $det(J_q) > 0$ for all $q \geq 0$, so Turing bifurcation does not occur. □

Theorem 3.5 *The reaction–diffusion system (1) does not exhibit Hopf bifurcation at the steady state E^* provided $\alpha + \beta < 1$.*

Proof. Hopf bifurcation requires $tr(J_q) = 0$ and $\det(J_q) > 0$ for some $q \geq 0$. From (12), the trace is

$$tr(J_q) = \mu(\alpha + \beta - 2) - (D_k + D_h)q^2.$$

Under $\alpha + \beta < 1$, we have $\mu(\alpha + \beta - 2) < 0$, while $(D_k + D_h)q^2 \geq 0$ for all $q \geq 0$. Therefore, $tr(J_q) < 0$ for all $q \geq 0$, and the condition $tr(J_q) = 0$ cannot be satisfied. Hence, Hopf bifurcation does not occur. □

The analysis shows that under $\alpha + \beta < 1$, diffusion shifts the spectrum J_{E^*} strictly into the stable half-plane for all $q > 0$, reinforcing rather than destabilizing the steady state. Convergence toward E^* is monotone at the modal level, as each Fourier mode $\epsilon_n(t)$ and $\eta_n(t)$ decays exponentially to zero, while the spatial profiles $k(x,t)$ and $h(x,t)$ may exhibit transient non-monotone behavior before approaching spatial homogeneity. Consequently, trajectories originating from a sufficiently small neighborhood of E^* converge to the homogeneous steady state E^*, representing a locally stable balanced growth path without spatial pattern formation or oscillatory behavior.

3.4 Numerical Simulations

Numerical simulations are conducted to illustrate the analytical stability results established in Section 3, and to visualize the spatiotemporal dynamics of physical capital (k) and human capital (h) within the spatial augmented Solow model. These simulations examine the local behavior of the positive steady state E^* in the presence of localized perturbations induced by heterogeneous initial capital endowments. The diffusion parameters D_k and D_h govern the spatial mobility of physical and human capital across the domain. The output elasticities α and β characterize the contribution of each type of capital to production, while μ represents the effective depreciation rate, which must be offset by the investment rates s_k and s_h to sustain positive capital accumulation.

To illustrate the local asymptotic stability of the non-spatial system established in Theorem 3.1, parameter values are chosen to satisfy the decreasing returns to scale condition $\alpha + \beta < 1$ and the positivity constraints $s_k, s_h, \alpha, \beta, \mu > 0$, while remaining consistent with plausible macroeconomic settings in the literature [9]. The output elasticities are set to $\alpha = 0.33$ and $\beta = 0.33$. The investment rates are $s_k = 0.20$ and $s_h = 0.15$, with physical capital investment slightly exceeding human capital expenditure. The effective depreciation rate is $\mu = 0.07$, representing moderate capital depreciation and population growth. Under these parameters, system (3) admits a unique positive homogeneous steady state at $E^* \approx (16.60, 12.45)$, consistent with the closed-form solution in Section 3.1. The phase plane of the non-spatial (k, h) dynamics is presented in Figure 2.

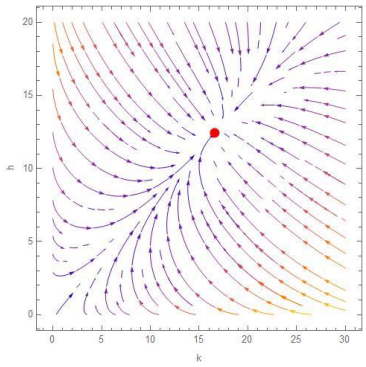

Figure 2. Phase plane at the steady state E^* with parameters $\alpha = 0.33$, $\beta = 0.33$, $s_k = 0.20$, $s_h = 0.15$, and $\mu = 0.07$

As shown in Figure 2, the displayed trajectories converge toward the steady state E^*. This confirms that regions with initially unequal capital endowments ultimately attain a uniform long-run growth rate, consistent with the local asymptotic stability established in Theorem 3.1.

To illustrate the spatial stability and bifurcation results of Sections 3.2 and 3.3, diffusion coefficients and localized shocks are introduced into the system. The diffusion parameters are set as $D_k = 0.05$ and $D_h = 0.10$, with $D_h > D_k$, reflecting that human capital diffusion, which includes knowledge spillovers in addition to skilled worker mobility, proceeds more rapidly than the relocation of physical capital [3, 4]. Small initial perturbations of magnitude $A_k = 0.50$ for k and $A_h = 0.40$ for h are applied, representing approximately 3% deviation from the respective steady state values $k^* \approx 16.60$ and $h^* \approx 12.45$. These perturbations simulate localized economic shocks, such as concentrated regional investments or labor migration, while remaining within the linearization regime required for the stability analysis of Section 3.2. The governing partial differential equations of system (1) are solved using a forward Euler finite-difference scheme with central differences in space, on a uniform spatial grid of $N = 50$ nodes on $[0, 50]$ with time step $\Delta t = 0.1$ and spatial step $\Delta x = 1.0$, integrated up to $T = 200$. The discretized system at each interior node i is given by

$$k_i^{n+1} = k_i^n + \Delta t \left[s_k (k_i^n)^\alpha (h_i^n)^\beta - \mu k_i^n + D_k \frac{k_{i+1}^n - 2k_i^n + k_{i-1}^n}{\Delta x^2} \right],$$

$$h_i^{n+1} = h_i^n + \Delta t \left[s_h (k_i^n)^\alpha (h_i^n)^\beta - \mu h_i^n + D_h \frac{(h_{i+1}^n - 2h_i^n + h_{i-1}^n)}{\Delta x^2} \right],$$

Homogeneous Neumann boundary conditions are imposed via ghost points by setting $k_{-1}^n = k_1^n$ and $k_{N+1}^n = k_{N-1}^n$ and analogously for h. The initial conditions are given by

$$k_0(x) = k^* + \varepsilon \cos(qx) \text{ and } h_0(x) = h^* + \delta \cos(qx),$$

representing localized perturbations of amplitude ε and δ about the steady state. The spatiotemporal outcomes for this representative parameter configuration are illustrated in Figure 3.

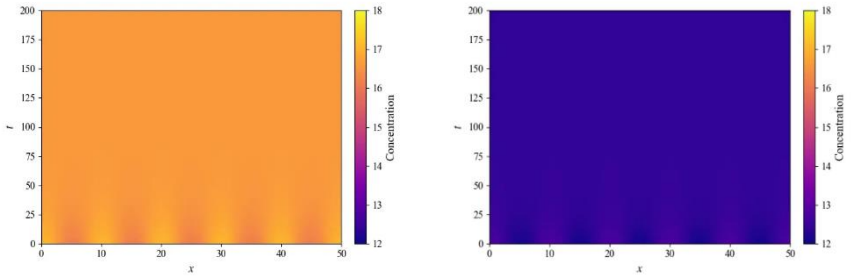

(a) (b)

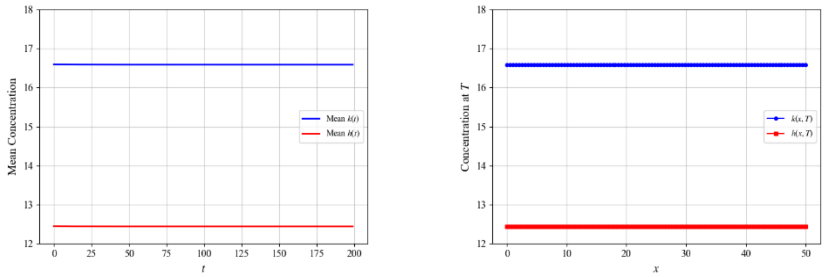

(c) (d)

Figure 3. Numerical simulation of the reaction–diffusion system (1) with parameters $\alpha = 0.33$, $\beta = 0.33$, $\mu = 0.07$, $s_k = 0.20$, $s_h = 0.15$, $A_k = 0.50$, $A_h = 0.40$, $D_k = 0.05$ and $D_h = 0.10$. (a) Spatiotemporal dynamics of physical capital $k(x,t)$. (b) Spatiotemporal dynamics of human capital $h(x,t)$. (c) Temporal evolution of the mean concentrations of k and h. (d) Spatial distribution of k and h at final simulation time $t = 200$

Figures 3(a) and 3(b) show that the initial localized perturbations are smoothed spatially over time, with no emergence of spatial patterns or oscillatory behavior. The diffusion terms gradually homogenize the capital distributions across the domain. Figures 3(c) and 3(d) further show that both the mean concentrations and the spatial profiles approach $k^* \approx 16.60$ and $h^* \approx 12.45$, with the final state exhibiting near-spatial homogeneity. These results are consistent with the local asymptotic stability predicted by the linearization analysis for the chosen parameter configuration. From a macroeconomic standpoint, the simulation suggests that, near the steady state, capital mobility does not generate spatial agglomerations under the present model structure.

4. CONCLUSION

This research establishes that the reaction–diffusion mechanism preserves the local asymptotic stability of the positive steady state $E^* = (k^*, h^*)$ of the spatial augmented Solow model. The non-spatial system is locally asymptotically stable under decreasing returns to scale $(\alpha + \beta < 1)$, and this stability is shown to persist when spatial diffusion of both physical and human capital is introduced. Diffusion shifts the spectrum of the spatial Jacobian further into the stable region, as reflected by a strictly negative trace and a strictly positive determinant for all nonnegative wave numbers. Bifurcation analysis confirms that neither Turing nor Hopf instabilities arise, so the balanced growth path remains stable under interregional capital flows. Consequently, for initial conditions in a neighborhood of the steady state, the joint mobility of physical and human capital supports convergence toward the homogeneous balanced growth path E^*, with each spatial mode decaying exponentially, while decreasing returns to scale preclude persistent spatial disparities and oscillatory behavior. For future research, the framework may be extended to nonlinear diffusion, heterogeneous saving rates, or cross-diffusion between capital types, potentially giving rise to richer spatial dynamics and conditions for regional agglomeration or divergence.

ACKNOWLEDGEMENTS

The authors gratefully acknowledge the reviewers for their careful evaluation and valuable suggestions, which have substantially improved the quality and clarity of this paper.

REFERENCES

[1] A. J. Scott and M. Storper, "Regions, globalization, development," *Regional Studies*, vol. 37, pp. 579–593, 2003.
[2] A. Faggian and P. McCann, "Human capital, graduate migration and innovation in British regions," *Cambridge Journal of Economics*, vol. 33, pp. 317–333, 2009.
[3] A. Kubis and L. Schneider, "Human capital mobility and convergence: A spatial dynamic panel model of the German regions," IWH Discussion Papers No. 9, Halle Institute for Economic Research, Halle, Germany, 2012.
[4] S. Iammarino, A. Rodríguez-Pose, and M. Storper, "Regional inequality in Europe: Evidence, theory and policy implications," *Journal of Economic Geography*, vol. 19, pp. 273–298, 2019.
[5] R. J. Barro and X. Sala-i-Martin, *Economic Growth*, 2nd ed. Cambridge: MIT Press, 2004.
[6] H. Uzawa, "Neutral inventions and the stability of growth equilibrium," *The Review of Economic Studies*, vol. 28, pp. 117–124, 1961.

[7] R. M. Solow, "A contribution to the theory of economic growth," *Quarterly Journal of Economics*, vol. 70, pp. 65–94, 1956.
[8] T. W. Swan, "Economic growth and capital accumulation," *Economic Record*, vol. 32, pp. 334–361, 1956.
[9] N. G. Mankiw, D. Romer, and D. N. Weil, "A contribution to the empirics of economic growth," *Quarterly Journal of Economics*, vol. 107, pp. 407–437, 1992.
[10] C. Camacho and B. Zou, "The spatial Solow model," *Economics Bulletin*, vol. 18, pp. 1–11, 2004.
[11] V. Capasso, R. Engbers, and D. La Torre, "On a spatial Solow model with technological diffusion and nonconcave production function," *Nonlinear Analysis: Real World Applications*, vol. 11, pp. 3858–3876, 2010.
[12] A. Xepapadeas and A. N. Yannacopoulos, "Spatial growth with exogenous saving rates," *Journal of Mathematical Economics*, vol. 67, pp. 125–137, 2016.
[13] G. C. González-Parra, B. M. Chen-Charpentier, A. J. Arenas, and M. Díaz-Rodríguez, "Mathematical modeling of physical capital diffusion using a spatial Solow model: Application to smuggling in Venezuela," *Economies*, vol. 10, p. 164, 2022.
[14] J. P. Juchem Neto, P. H. de Almeida Konzen, and J. C. Ruiz Claeyssen, "A model of economic growth in two spatial dimensions," in *Proceedings of SBMAC*, vol. 10, 2023.
[15] M. M. Fischer, "A spatial Mankiw–Romer–Weil model: Theory and evidence," *The Annals of Regional Science*, vol. 47, pp. 419–436, 2011.
[16] B. Aymard, "Bifurcation analysis and steady state patterns in reaction–diffusion systems augmented with self- and cross-diffusion," *International Journal of Bifurcation and Chaos*, vol. 33, 2022.
[17] N. Ureña and A. M. Vargas, "On the numerical solution to a Solow model with spatial diffusion and technology-induced capital mobility," *Engineering Analysis with Boundary Elements*, vol. 157, pp. 541–552, 2023.
[18] Y. Zhong and W. Huang, "Spatial dynamics for a generalized Solow growth model," *Discrete Dynamics in Nature and Society*, vol. 2018, 2018.
[19] Y. Zhong, "The dynamics of a spatial economic model with bounded population growth," *Discrete Dynamics in Nature and Society*, vol. 2021, pp. 1-11, 2021.
[20] F. Kong, J. Sun, and S. Xie, "Stability and slow dynamics of an interior spiky pattern in a one-dimensional spatial Solow model with capital-induced labor migration," *arXiv:2510.19204*, 2025. [Online]. Available: https://arxiv.org/abs/2510.19204
[21] C. Li, X. Yuan, and Y. Gong, "Dynamic analysis of a Solow-Swan model with capital-induced labor migration," *Mathematics and Computers in Simulation*, vol. 234, pp. 73–85, 2025.
[22] F. Fabião, "Solow model, an economic dynamical system of growth," *Applied Mathematical Sciences*, vol. 3, pp. 2867–2880, 2009.
[23] S. Sutrima and R. Setiyowati, "Properties of solutions and stability of a diffusive wage-employment system," *Nonlinear Dynamics and Systems Theory*, vol. 23, pp. 434–446, 2023.
[24] S. Sutrima, R. Setiyowati, and M. Mardiyana, "Lotka-Volterra system of predator-prey type with time-dependent diffusive," *Results in Nonlinear Analysis*, vol. 7, pp. 27–42, 2024.
[25] A. L. Krause, E. A. Gaffney, P. K. Maini, and V. Klika, "Modern perspectives on near-equilibrium analysis of Turing systems," *Philos. Trans. R. Soc. A*, vol. 379, p. 20200268, 2021.
[26] J. D. Murray, *Mathematical Biology II: Spatial Models and Biomedical Applications*, 3rd ed. New York, NY, USA: Springer, 2003.